INTERNATIONAL JOURNAL OF CLIMATOLOGY
Int. J. Climatol. **34**: 742–750 (2014)
Published online 9 May 2013 in Wiley Online Library
(wileyonlinelibrary.com) DOI: 10.1002/joc.3718

RMetS
Royal Meteorological Society

Diurnal cycle of summer rainfall in Shandong of eastern China

Hong Zhuo,[a] Ping Zhao[a]* and Tianjun Zhou[b]

[a] *State Key Laboratory of Severe Weather, Chinese Academy of Meteorological Sciences, Beijing 10081, China*
[b] *LASG, Institute of Atmospheric Physics, Chinese Academy of Sciences, Beijing 100029, China*

ABSTRACT: Using the hourly precipitation data at 123 gauge stations of Shandong province in eastern China during 1996–2008, the authors examine the spatial distribution of summer (June–July–August) precipitation amount (PA), precipitation intensity (PI), and precipitation frequency (PF) and their diurnal cycles. The results show that the diurnal peak of PA decreases from the southeastern to northwestern Shandong and mainly appears in the early morning and afternoon. The large diurnal peak of PA mainly appears in a large area from the hilly areas of southern Shandong to the eastern coasts. Large diurnal peak of PI mainly appears along the lower reaches of the Yellow River in northern Shandong. The diurnal peak of PF also decreases from southeastern to northwestern Shandong. The diurnal cycles of PA and PI have two peaks and they occur in the early morning and the afternoon, respectively. The diurnal cycle of PF has one peak in the morning. Large PA values show a southwestward time delay over northwestern Shandong, a northeastward time delay over central and southeastern Shandong in the afternoon, and a southeastward time delay over central and southeastern Shandong in the morning. Moreover, they also show a time delay from the central mountains of Shandong to its adjacent areas in the afternoon. When hourly precipitation is weaker, the diurnal cycles of PA and PF show a two-peak feature. With following the increase of hourly precipitation, the diurnal peak number also tends to increase.

KEY WORDS diurnal cycle; summer precipitation; Shandong of eastern China; climatic characteristics

Received 13 June 2011; Revised 10 April 2012; Accepted 30 March 2013

1. Introduction

Since diurnal cycle features of precipitation amount, precipitation intensity, and precipitation frequency are important to reveal changes of soil moisture, runoff, evaporation, and sensible heat flux over land (Qian *et al.*, 2006), investigating diurnal cycle features of precipitation is helpful not only to understand physical processes of precipitation formation but also to evaluate the capability of weather and climate models in simulating and forecasting temporal and spatial features of precipitation (e.g. Dai et al., 1999a, 1999b; Lin *et al.*, 2000; Yang and Slingo, 2001; Betts and Jakob, 2002; Dai and Trenberth, 2004; Liang *et al.*, 2004; DeMott *et al.*, 2007).

In recent years, diurnal cycles of precipitation have become one of hot topics in climate research (e.g. Dai, 2001a, 2001b, 2007; Trenberth *et al.*, 2003; Sun *et al.*, 2006, 2007; DeMott *et al.*, 2007). Many precipitation observations, including hourly rain gauge records and satellite measurements, have been extensively applied in studying diurnal cycles of precipitation over the East Asian monsoon region (Yu *et al.*, 2007a, 2007b; Li *et al.*, 2008; Zhou *et al.*, 2008). For example, Yu *et al.* (2007a) analyzed the characteristics of diurnal variations in summer precipitation over China. Their results showed that there are two comparable diurnal peaks for summer precipitation over the region between the Yangtze and Yellow Rivers. One appears in the early morning and another appears in the late afternoon. Zhou *et al.* (2008) confirmed these results and found that the diurnal cycle of precipitation amount is determined by both the precipitation intensity and precipitation frequency. They also found that the satellite measurement can only capture the later afternoon peak of precipitation in the regions between the Yangtze and Yellow Rivers. Yuan *et al.* (2010) further examined the intraseasonal characteristics of diurnal cycles of precipitation over eastern China in June to September, finding that the intraseasonal movement in the early morning peak of rainfall is associated with a shift of the East Asian monsoon rain band. Chen *et al.* (2010) addressed that the eastward time delay of rainfall diurnal peak along the Yangtze River is closely related to the diurnal evolution of the low-level southwesterly winds.

Although studies on precipitation diurnal variations over eastern China have made great progress, a number of questions remain unanswered. For example, because the previous studies used observations at the limited meteorological stations and lacked precipitation data with a higher spatial resolution, their results showed

* Correspondence to: P. Zhao, State Key Laboratory of Severe Weather, Chinese Academy of Meteorological Sciences, Beijing 100081, China.
E-mail: zhaop@cma.gov.cn

some regional differences on precipitation diurnal variations over China. Moreover, although there are some researches on terrain influences on diurnal cycles of precipitation (e.g. He and Zhang, 2010; Yin *et al.*, 2011; Sun and Zhang, 2012), they paid little attention to diurnal cycles with different rainfall intensity in the coasts, the inland areas, the hilly areas, the mountainous areas, and the plains of China by using hourly precipitation data. Therefore, it is useful to analyze diurnal cycles of different precipitation intensity (such as 0.1–10 mm h^{-1}, and 10–25 mm h^{-1}, and so on) to understand local climate and to validate precipitation parameterization schemes in weather and climate models.

Shandong province, located in the lower reaches of the Yellow River (114.3°E–122.7°E, 34.4°N–38.4°N) of eastern China (shown in Figure 1(a)), is a suitable region for comparing diurnal cycles of precipitation among the coasts, the inland areas, the hilly areas, the mountainous areas, and the plains. As shown in Figure 1(b), terrain in Shandong province is complicated and it consists of a central mountainous area such as Meng Mountain and Tai Mountain, the northern and southwestern plains in Shandong, the coasts in eastern Shandong, and some hilly areas. Under such a complicated terrain, how are the spatial distribution of hourly precipitation and the diurnal cycles with different rainy intensities during summer? With this question in mind, in this study, we use the dense hourly rainfall data at 123 meteorological stations of Shandong province to examine diurnal cycles of summer precipitation when East Asian summer monsoon (EASM) prevails over eastern China (Zhou and Yu, 2005; Zhao *et al.*, 2007).

The rest of this paper is organized as follows. The datasets and analysis methods are described in Section 2. The temporal and spatial distributions of precipitation amount, intensity, and frequency diurnal peaks are examined in Section 3. The diurnal variations of precipitation amount, intensity, and frequency and their regional differences are compared in Section 4 and the spatial varying features of diurnal cycles in precipitation amount are analyzed in Section 5. Regional diurnal cycles of precipitation amount, intensity, and frequency with different precipitation grades are discussed in Section 6. Finally, a summary and discussion are given in Section 7.

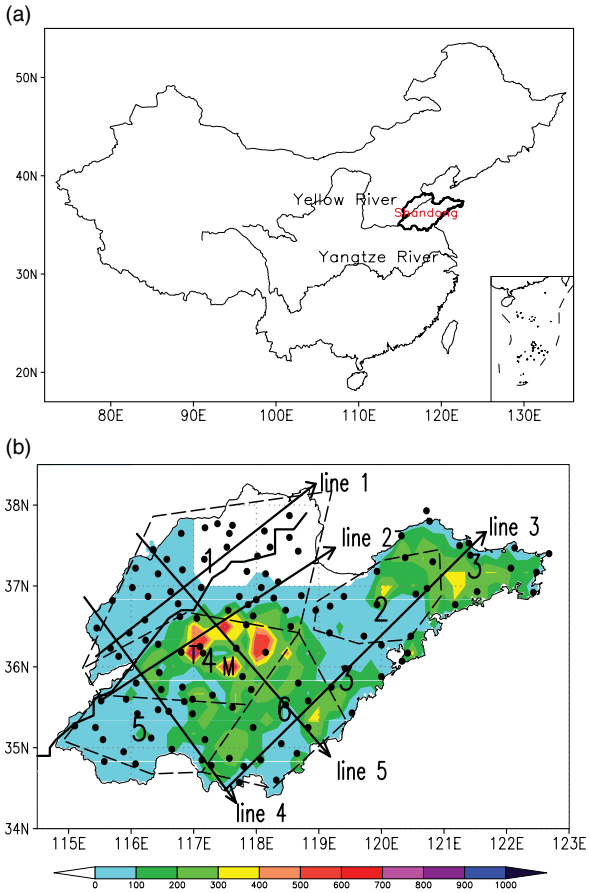

Figure 1. (a) Location of Shandong province in China, in which thick solid line indicates Shandong province; thin solid lines inside the mainland of China are for the Yangtze River and the Yellow River; and (b) the topography (colour shaded areas; unit: m) in Shandong, in which black dots indicate 123 rain-gauge stations, thick black solid line denotes the Yellow River, six regions are indicated by long dashed lines with their numbers inside the regions, five solid lines with an arrow indicate five cross sections in turn, and *M* and *T* indicate Meng Mountain and Tai Mountain.

2. Data and methods

The precipitation data with a temporal resolution of 1 h, automatically recorded by siphon or tipping-bucket rain gauge at 123 surface meteorological stations of Shandong (shown in Figure 1(b)), come from Shandong Meteorological Bureau of China. Among these stations, 96 stations have records during 1996–2008, 24 stations have records during 1999–2008, 2 stations have records during 2000–2008, and 1 station has records during 2001–2008. The quality of the precipitation records is assessed by using the extreme values of precipitation and the consistency among the precipitation records like Yu *et al.* (2007b). The gridded topographic elevation data with a horizontal resolution of 10′ are downloaded from the website (http://www.mmm.ucar.edu/wrf/OnLineTutorial/Basics/GEOGRID/ter_data.htm).

The observational data at rain gauge stations are interpolated onto regular grid points with a horizontal resolution of 0.11° in latitude and longitude. Consistent with Dai et al. (1999b) and Zhou *et al.* (2008), measurable precipitation is defined as larger than 0.1 mm h^{-1}. For each hour in a day, precipitation amount (PA) is defined as the climatological (1996–2008) average of summer (June–July–August, JJA) accumulated hourly precipitation divided by 92 days, precipitation intensity (PI) is defined as the climatological average of JJA accumulated hourly precipitation divided by measurable precipitation days during JJA, and precipitation frequency (PF) is defined as PA divided by PI.

In this study, a day (24 h) is divided into four periods. They are 0800–1400 Beijing Time (BT) (0000–0600 UTC), 1400–2000 BT (0600–1200 UTC), 2000–0200 BT (1200–1800 UTC), and 0200–0800 BT (1800–2400

UTC), in which BT is for Beijing time. Following the previous studies (Dai *et al.*, 1999; Liang *et al.*, 2004; Yu *et al.*, 2007a, 2007b; Zhou *et al.*, 2008), the occurring time of diurnal precipitation peak is indicted by an arrow pointer on a circular 24-h dial clock. For example, an eastward vector indicates that the maximum value occurs at 0800 BT (0000 UTC). Note since the zonal coverage of Shandong province is less than 15°, BT rather than local solar time is used here.

3. Spatial and temporal features of PA, PF, and PI diurnal peaks

In this section, we used the hourly peak PA/PF/PI (hereafter PPA/PPI/PPF) in a day (24 h) to reveal spatial and diurnal cycle features of PA/PI/PF. Figure 2(a) shows the horizontal distributions of PPA and its occurrence time. Generally speaking, large PPA values appear in a large region from the hilly area of southern Shandong to the eastern coasts, corresponding to the prevailing southwesterly monsoon flow (Zhao *et al.*, 2007). Meanwhile, PPA gradually decreases from southeastern to northwestern Shandong, which corresponds to the weakening of the southeasterly flow from the coasts of Shandong to the inland areas (Tao and Chen, 1987). The large PPA above 0.34 mm h^{-1} appears on the southeastward slope of Meng Mountain (indicated by A), on the southwestward slopes of Meng and Tai Mountains (indicated by B and C, respectively), in the hilly areas of southern Shandong (indicated by D), in the southeastern coasts of eastern Shandong (indicated by E, F, and G), and near the peak of Tai Mountain (indicated by H). The PPA below 0.2 mm h^{-1} mainly appears in the northwestern plains of Shandong and goes in the southwest–northeast direction. Moreover, the low PPA also appears at the lee sides of Meng and Tai Mountains.

Different from the distribution of PPA, the large PPI above 4.4 mm h^{-1} mainly appears at the windward sides of the mountainous and hilly areas of Shandong and goes generally in the southwest–northeast direction along the lower reaches of the Yellow River (Figure 2(b)). Moreover, large PPI also appears in the northern coasts of eastern Shandong, with its centre near 37.2°N, 120.2°E. The PPI below 2.8 mm h^{-1} appears on the northeastern slope of Meng Mountain and in the northwestern plains of Shandong.

Similar to the PPA, there are large PPF values in southeastern Shandong and PPF generally decreases from southeastern to northwestern Shandong. Low PPF values appear in northwestern Shandong and goes in the southwest–northeast direction (Figure 2(c)).

It is also noted from Figure 2(a) that PPA occurs in the early morning in the hilly areas of southeastern Shandong, in the central mountainous areas, and in the eastern coasts (Figure 2(a)). In other regions, PPA mainly occurs in the early morning or the afternoon, which is possibly due to different prevailing precipitation systems. PPI occurs in the eastern coasts and southeastern hilly areas of Shandong in the morning and mainly occurs in other regions in the late afternoon (Figure 2(b)). For most of Shandong, PPF mainly occurs in the early morning (Figure 2(c)).

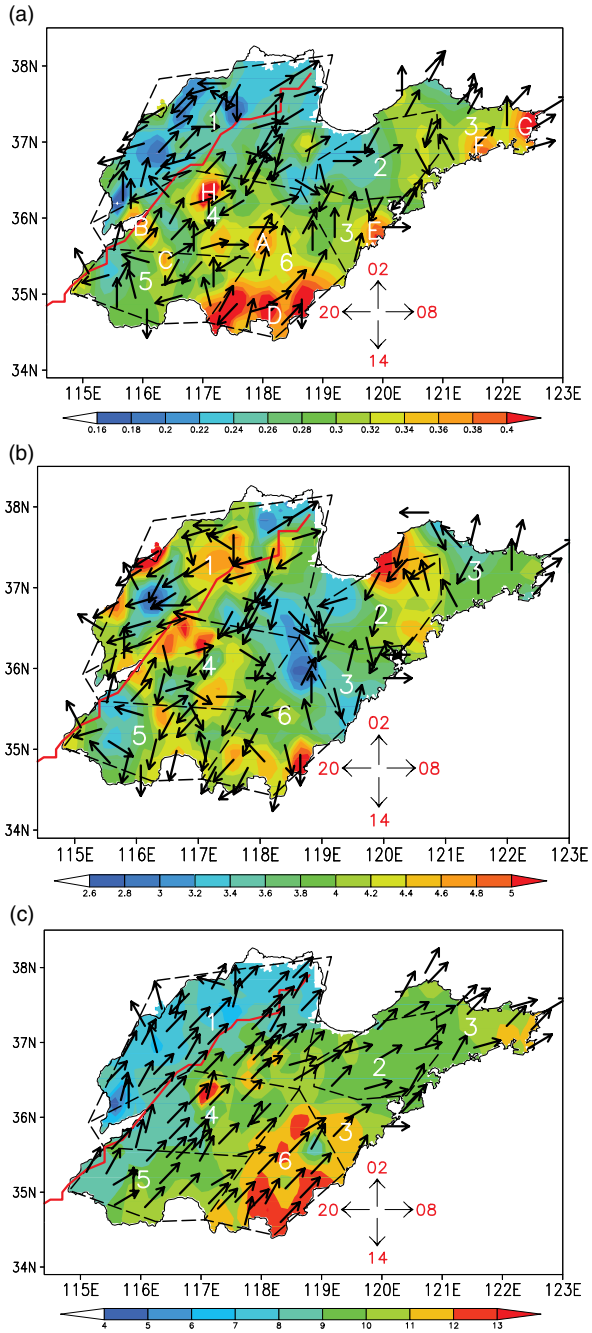

Figure 2. (a) Horizontal distribution of summer PPA (colour shaded areas; mm h^{-1}) and its occurrence time (arrow) in a day (24 h); (b) same as in (a) but for PPI; (c) same as in (a) but for PPF (%). BT is indicated by a phase clock, the Yellow River is indicated by the thick solid red line, and six regions are indicated by long dashed lines.

4. Diurnal cycles of regional mean PA, PI, and PF

Figure 3 shows the diurnal cycles of regional mean PA, PI and PF over Shandong. In the figure, there are two peaks for PA and PI. For PA, one larger peak occurs around

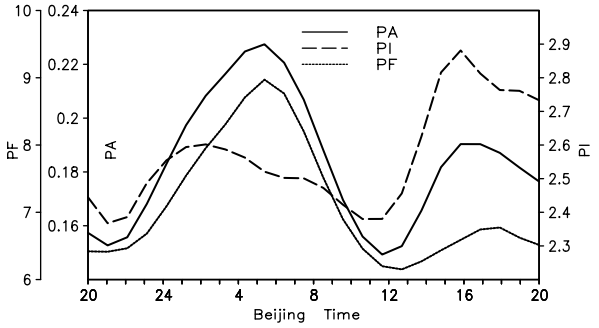

Figure 3. Diurnal cycles of summer PA ($mm\,h^{-1}$, solid line), PI ($mm\,h^{-1}$, dashed line), and PF (%, dotted line) averaged over Shandong province. The x-axis is for BT (unit: h).

0500 BT (2100 UTC) and another lower peak occurs around 1600 BT (0800 UTC). For PI, one larger peak occurs around 1600 BT (0800 UTC), with another smaller peak around 0200 BT (1800 UTC). PF has only one peak and it occurs around 0500 BT (2100 UTC). Based on the definition in Section 2, PA may be determined by both PI and PF. When precipitation is moderate but frequent (such as monsoon precipitation) or lasts for a short-time but with large intensity (such as convective precipitation), PA is larger. Thus the bigger peak of PA around 0500 BT (2100 UTC) is possibly determined by PF while the smaller peak around 1600 BT (0800 UTC) is possibly determined by PI. This result further supports the conclusion of Zhou *et al.* (2008). Their study addressed that the diurnal variation of PA can be attributed to PI and PF over most of eastern China.

Following Yu *et al.* (2007a) and Zhou *et al.* (2008), we further divide Shandong into six regions (shown in Figure 1(b)) on the basis of the occurring time of PPA (in Figure 2(a)) and the terrain distribution in Shandong (in Figure 1(b)). Figure 4 shows diurnal cycles of PA, PI, and PF for each region. It is evident that PA has a peak in the early morning for six regions, which possibly reflects an effect of dominant large-scale monsoon precipitation, while another peak appears in the afternoon (1500–2000 BT) (on the left of Figure 4), which suggests an effect of the local thermally induced convective precipitation. Moreover, the morning PA peak exceeds $0.25\,mm\,h^{-1}$ in region 3 (the eastern coasts), region 4 (the central mountainous areas), and region 6 (the southeastern hilly areas), while it is generally small (between 0.1 and $0.2\,mm\,h^{-1}$) in region 1 (the northern plains) and region 2 (the inland area of eastern Shandong). Compared to the morning PA peak, the afternoon PA peak is comparable in magnitude in regions 1, 2, and 5 (the southwestern plains) and is smaller in regions 3, 4, and 6, which is similar to the result of Zhou *et al.* (2008) and Dai (2001b, 2007). Their studies showed that the PA peak often appears in the early morning rather than the afternoon in the Yellow River and over the adjacent oceans. For PI (in the middle of Figure 4), a pronounced peak of PI with $2.8–3.0\,mm\,h^{-1}$ occurs in the late afternoon (1500–1700 BT) for each region, which possibly indicate an effect of the local convective activities triggered by surface heat flux from solar radiation in the late afternoon. Meanwhile, another peak with $2.7–3.1\,mm\,h^{-1}$ occurs in the late night (between the midnight and 0400 BT) for regions 2, 3, 4, 5, and 6. One peak of PF mainly appears in the early morning (0500–0600 BT) for each region (on the right of Figure 4). This consistence in the occurrence time of the PF peak among the different regions may reflect an effect of large weather systems. Another weaker peak occurs in the afternoon (1800 BT) for regions 1, 4, and 5, which possibly indicates an effect of local convection activities.

5. Spatial feature of PA diurnal cycle

On the basis of the spatial features of PPA in the southeast–northwest or southwest–northeast directions (shown Section 3), we select lines 1–5 in the southwest–northeast or southeast–northwest direction (shown Figure 1(b)) to further examine the spatial features of PA diurnal cycles in different horizontal directions. Here, lines 1, 2, and 3 generally pass respectively through the northwestern, central, and southeastern parts of Shandong in the southwest–northeast direction, consistent with the direction of prevailing southwesterly winds, and lines 4 and 5 pass respectively through the southwestern and central parts of Shandong in the northwest–southeast direction, opposite to the direction of local southeasterly winds.

Figure 5(a) shows the temporal cross section of the PA diurnal cycle along line 1. In the figure, the PA above $0.2\,mm\,h^{-1}$ first appears in position A in the afternoon (around 1600 BT), in position B at 1800 BT, and in position C at 2100 BT, which suggests a southwestward time delay of large PA in the northern plains of Shandong. When we change the time-axis from 2000 to 2000 BT, this southwestward time delay in the afternoon is still observed (figure not shown). The time delay of PA in the morning is not remarkable because it occurs almost simultaneously along line 1, which indicates a synchronously varying feature of PA. Along line 2 (Figure 5(b)), the PA above $0.26\,mm\,h^{-1}$ appears in position A (on the northern slope of Tai Mountain) around 1500 BT, in position B near 1600 BT, which indicates a northeastward time delay possibly due to valley breeze (Qian, 2008; Qian *et al.*, 2010). The similar phenomenon also occurs in position C around 1800 BT and in position D after 2 h. Moreover, in the morning, the large PA in Tai Mountain shows a synchronously varying feature.

Along line 3 (Figure 5(c)), the temporal evolution of PA is complicated. Over region 6, the PA above $0.28\,mm\,h^{-1}$ generally shows a northeastward time delay, for example, from position A via position B to position C in the morning and from position D to position E in the afternoon. This time delay corresponds to the local prevailing southwesterly monsoon. In regions 2 and 3, large PA first appears in position F (on the windward side of hills in eastern Shandong) around 1300 BT, in position G around 1500 BT, and in position H around 1600 BT,

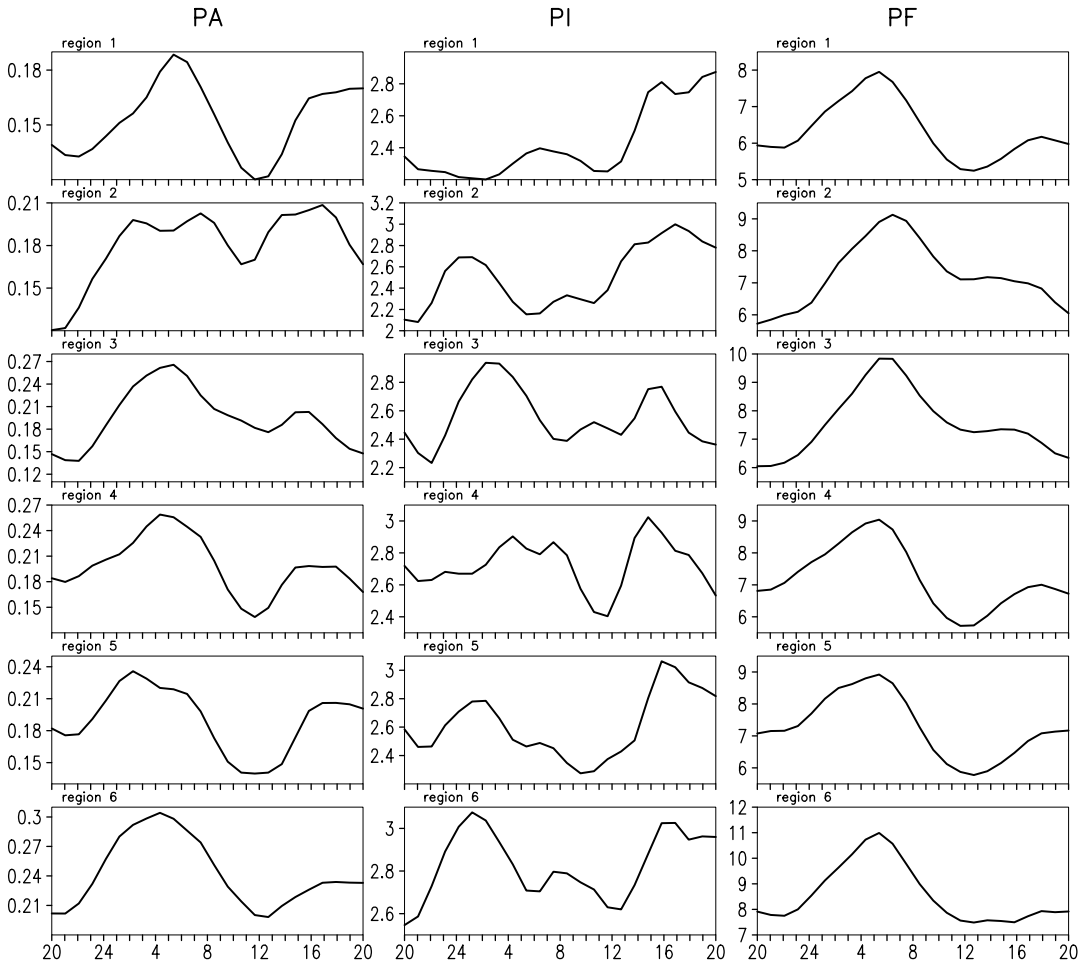

Figure 4. Same as in Figure 3 but for PA (left), PI (middle), and PF (right) in six regions.

which indicates a northeastward time delay. Meanwhile, large PA also emerges in position I (to the northeast of Shandong southeastern hills) around 1500 BT, which indicates a southwestward time delay from position F. These northeastward and southwestward time delays in regions 2 and 3 possibly reflect effects of the valley-breeze and sea-breeze convergence in the afternoon that may enhance local convection (Qian, 2008; Qian *et al.*, 2010). Similarly, large PA also occurs in positions J and K around 0200 BT and 0500 BT, respectively, and then moves to position L around 0800 BT, which possibly indicates effects of land and mountain breezes (Qian, 2008; Qian *et al.*, 2010).

In the northwest-southeast direction, along line 4 (Figure 5(d)), the PA above 0.24 mm h^{-1} emerges in regions 5 and 6 from 0100 to 1200 BT, which indicates a southeastward time delay in the morning. In the afternoon, the large PA appears in region 6 around 1500 BT and in region 5 around 1700 BT. This result indicates a northwestward time delay. Along line 5 (Figure 5(e)), the PA above 0.26 mm h^{-1} in the morning emerges earlier in region 6 than in region 4. Moreover, it occurs in region 4 at 1500 BT and to the southeast of this region at 1700 and 1900 BT, which indicates a time delay from the central mountains to its adjacent areas.

6. Diurnal cycles of PA, PI, and PF with different precipitation intensity

In this section, hourly precipitation is also divided into four grades, that is, 0.1–10 mm h^{-1}, 10–25 mm h^{-1}, 25–50 mm h^{-1}, and 50–100 mm h^{-1}, and precipitation above 100 mm h^{-1} is not discussed because it scarcely occurs. For each precipitation grade, PA, PF, and PI are calculated using the corresponding hourly precipitation. We examine diurnal cycles of PA, PI, and PF corresponding to four grades of hourly precipitation for each region.

Figure 6 shows diurnal variations of regional mean PA in each region for each grade of hourly precipitation. When hourly precipitation is 0.1–10 mm h^{-1}, the PA diurnal cycle shows a noticeable peak in the early morning for regions 1–6 and a weaker peak in the late afternoon for regions 1, 2, 4, and 5 (Figure 6(a)). When hourly precipitation is 10–25 mm h^{-1} (Figure 6(b)), the PA diurnal variation has two peaks in six regions. One appears in the early morning and another appears in the late afternoon. The early morning peak is bigger in regions 3, 4, and 6. In regions 1, 2 and 5, the late afternoon peak is generally comparable to the early morning peak. When hourly precipitation is 25–50 mm h^{-1} (Figure 6(c)), there are two peaks in regions 3 and 4. One appears in the morning and another appears in the late afternoon. There

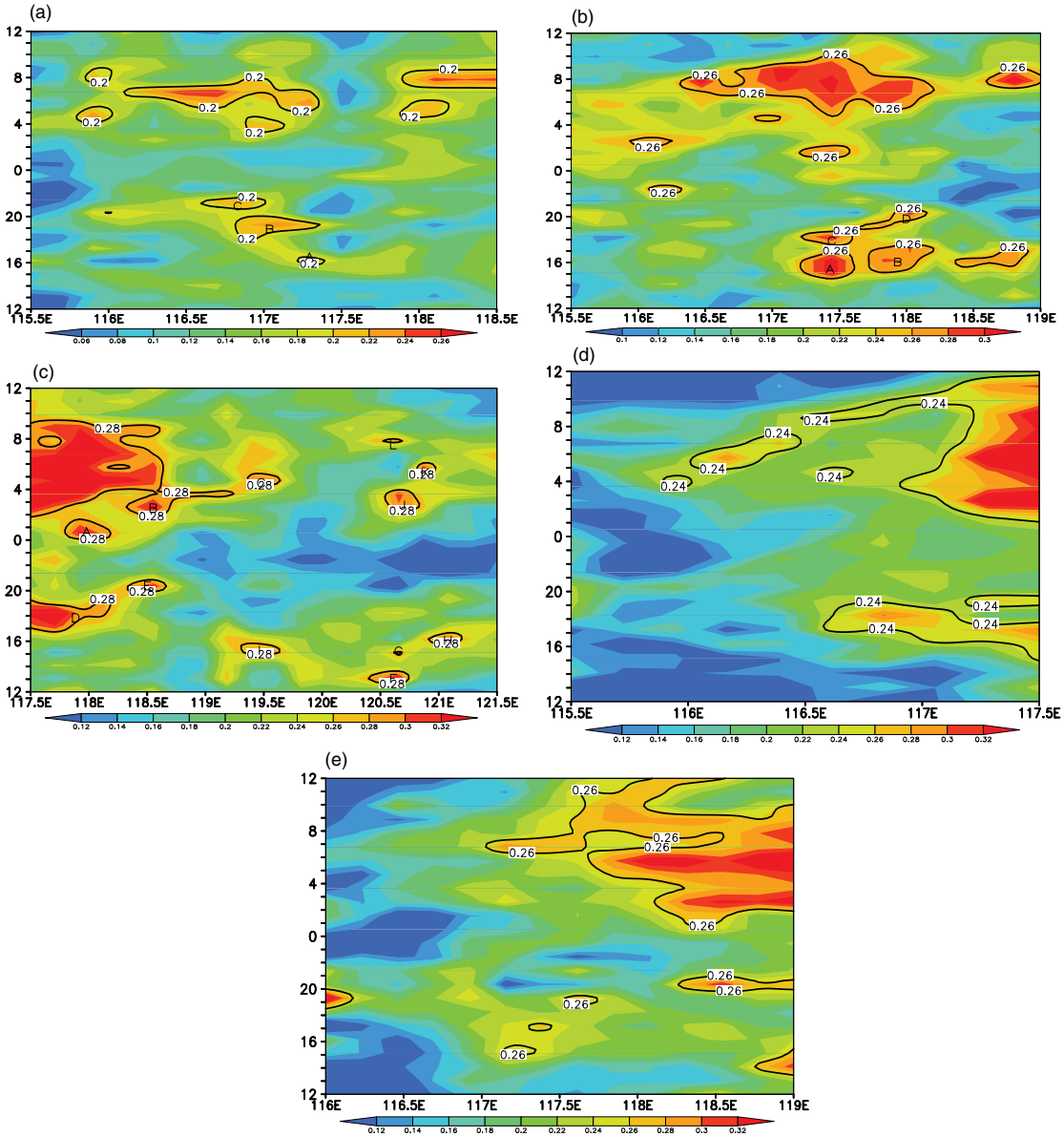

Figure 5. (a) Temporal cross section of summer PA (mm h^{-1}) along line 1, in which the vertical axis is for BT (unit: h); and (b) to (e) same as (a) but along lines 2 to 5, respectively.

are generally three peaks in regions 1, 2, and 6. The PA is larger in the afternoon than in the morning in regions 1 and 2 and is larger in the morning than in the afternoon in region 6. For region 5, there are four peaks and they appear respectively at midnight, in the early morning, in the morning, and in the late afternoon, with a large peak at midnight and in the late afternoon. When hourly precipitation reaches 50–100 mm h^{-1} (Figure 6(d)), PA has at least three peaks for each region and the morning peak is comparable to the afternoon peak in regions 1, 2, 4, 5, and 6 while the morning peak is more prominent relative to the afternoon peak in region 3. It is evident that the PA peak numbers tend to increase following the increase of hourly precipitation amount.

Figure 7 shows diurnal cycles of regional PI for four precipitation grades. Generally speaking, PI has more than two peaks in most regions for four precipitation grades. In region 1, the morning PI peaks are comparable to the afternoon peaks when hourly precipitation is 0.1–10 mm h^{-1} or 10–25 mm h^{-1}. The afternoon peak becomes more prominent relative to the morning peak when hourly precipitation reaches 25–50 mm h^{-1}, which possibly reflects an influence of local heavy-rainfall weather systems. When precipitation enhances to 50–100 mm h^{-1}, the morning peak becomes significant again and matches to the afternoon peak, which may suggests an effect of southwest monsoon on heavy precipitation in the northern plain of Shandong. In region 2 (the inland area of eastern Shandong), the morning peak is comparable to the afternoon peak when hourly precipitation is 0.1–10 mm h^{-1} or 10–25 mm h^{-1}. When precipitation reaches 25–50 mm h^{-1} or 50–100 mm h^{-1}, the afternoon peak becomes stronger relative to the morning peak, which is possibly associated with the

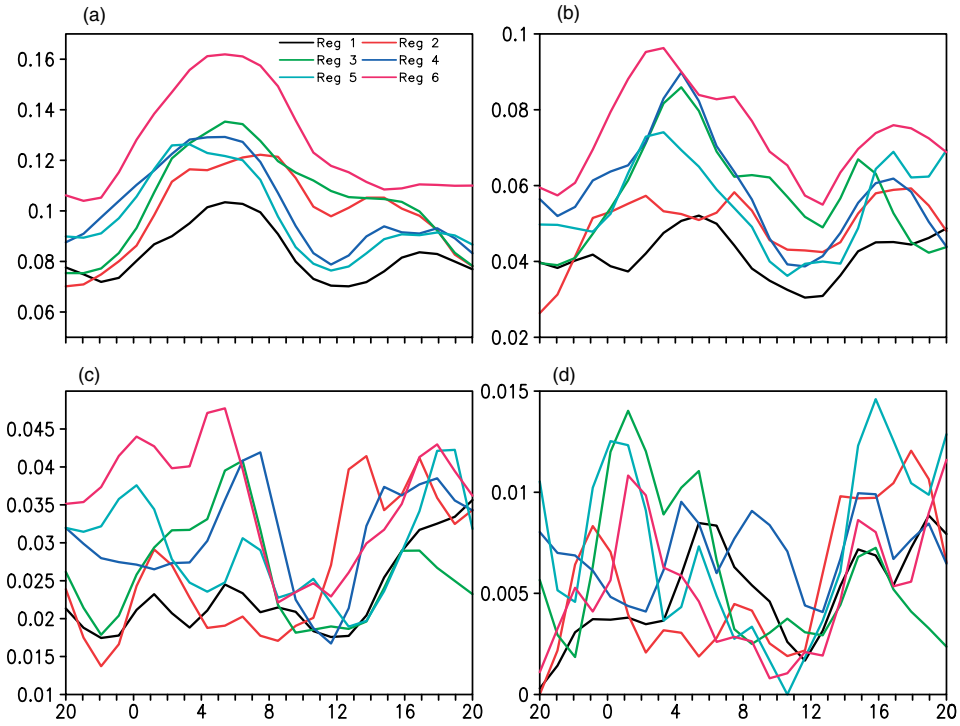

Figure 6. Diurnal cycles of PA averaging over six regions for (a) 0.1–10 mm h^{-1}, (b) 10–25 mm h^{-1}, (c) 25–50 mm h^{-1}, and (d) 50–100 mm h^{-1}. The horizontal axis is for BT (unit: h).

low-level sea-breeze convergence that may enhance precipitation in the afternoon in a narrow area of eastern Shandong (Qian, 2008; Qian *et al.*, 2010). In region 3, the morning peak is also comparable to the afternoon peak when precipitation is 0.1–10 mm h^{-1} or 10–25 mm h^{-1}. The peak becomes more remarkable in the morning than in the afternoon when precipitation is 25–50 mm h^{-1} or 50–100 mm h^{-1}, which suggests a dominant monsoon precipitation over the eastern coasts. For regions 4, 5, and 6, there are more than two comparable PI peaks for four precipitation grades, which may reflect a mixed role of monsoon and convective precipitations in the mountainous area, the southwestern plain, and the southeastern hills of Shandong.

In addition, we also examine the diurnal cycles of PF for each precipitation grade and find that for six regions the features of PF diurnal cycles are similar to those of PA except in magnitude (figures not shown).

7. Summary and discussion

7.1. Summary

Using hourly precipitation data with a high spatial resolution at 123 gauge stations of Shandong in eastern China during 1996–2008, we have examined the spatial distributions of summer PA, PI, and PF and their diurnal cycles. The results show that the PA peak gradually decreases from southeastern to northwestern Shandong and mainly appears in the early morning or the afternoon. Large PA peaks generally appear in a large region from the hilly area of southern Shandong to the eastern coasts while low PA peaks mainly appear in the northwestern plains. This spatial pattern is possibly associated with the local prevailing monsoon flow. Large PI peaks mainly appear along the lower reaches of the Yellow River and low PI peaks mainly appear on the lee sides of the central mountainous areas and in the northwestern plains of Shandong. Moreover, large PI peaks appear over most of Shandong in the late afternoon except in the hilly areas and the eastern coasts in the morning. The PF peak generally decreases from southeastern to northwestern Shandong, with large PF peaks in southwestern Shandong and low PF peaks in the northwestern part. Large PF appears over most of Shandong in the early morning.

The provincially and regionally averaged diurnal cycles of both PA and PI generally show a two-peak feature. PA (PI) has a stronger (weaker) peak in the early morning and a weaker (stronger) peak in the afternoon. PF has only one peak in the morning. Over the northwestern Shandong, large PA shows a southwestward time delay in the afternoon and a synchronously varying feature in the morning (without a remarkable time delay). Over the central and southeastern Shandong, large PA mainly shows a northeastward time delay in the afternoon. In the northwest-southeast direction, large PA exhibits a southeastward time delay over central and southeastern Shandong in the morning and a time delay from the central mountains of Shandong to its adjacent areas in the afternoon.

The relationship between precipitation diurnal cycle and intensity is complicated in Shandong. When hourly precipitation is weaker (0.1–10 mm h^{-1} or

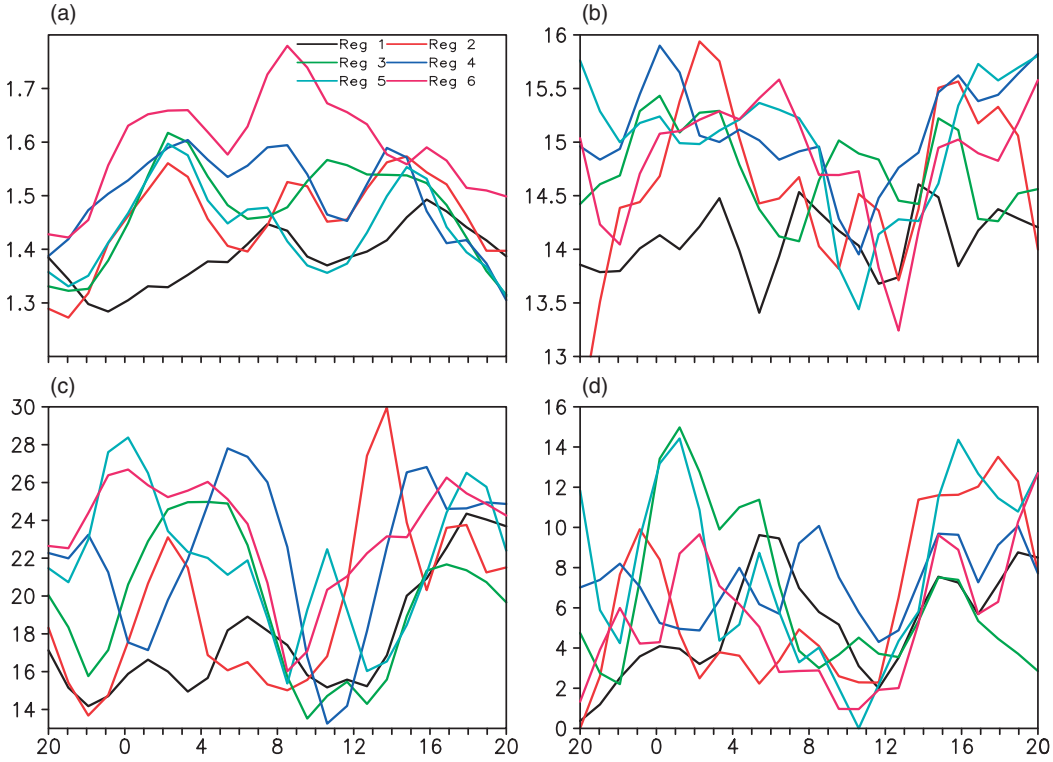

Figure 7. Same as in Figure 6 but for PI.

10–25 mm h^{-1}), the diurnal cycles of PA and PF mainly show a two-peak feature. One appears in the morning and another appears in the afternoon. The number of precipitation peak tends to increase with an increase of hourly precipitation. When hourly precipitation reaches 50–100 mm h^{-1}, PA usually has at least three peaks. Compared to PA and PF, PI has generally more peaks, and its afternoon peaks become more prominent and are comparable to the morning peaks when precipitation enhances.

7.2. Discussion

Previous studies have showed that land–sea breezes often play an important role in tropical precipitation and precipitation usually occurs earlier near the coasts, gradually propagating toward the inland areas (Qian, 2008; Qian *et al.*, 2010). Although Shandong is located in the middle latitude, it neighbours the western North Pacific. Thus the effects of land–sea breezes on precipitation in Shandong may be similar to those in the tropics. When breezes from seas converge toward the inland areas of Shandong, precipitation increases in the inland areas in the afternoon, which may enhance the afternoon peak of precipitation (shown in Figures 6 and 7). Our analysis also shows that the PA afternoon peak appears earlier in the northern plain near sea than in the central northern plain (shown in Figure 5(a)). Moreover, mountain and valley breezes also modulate diurnal cycles of precipitation (Qian, 2008; Qian *et al.*, 2010). Our result shows that in Tai Mountain, the afternoon precipitation peak may enhance because of the convergence caused by valley breezes (shown in Figure 4) and then move to the adjacent areas (shown in Figure 5(b) and (e)).

Because Shandong is located in the northern part of East Asian summer monsoon region, Shandong precipitation is subject to major monsoon systems (such as the subtropical ridge over the western North Pacific). Following the seasonal cycle of East Asian summer monsoon, when Shandong is located to the west or north of the subtropical ridge, the southeast or southwest monsoon prevails over Shandong (Zhou *et al.*, 2009). Previous studies addressed that the interactions between monsoon and topography may enhance local precipitation (Chang *et al.*, 2005). Thus, corresponding to the prevalence of summer southwest or southeast monsoon in Shandong, large peaks of PA, PI, and PF and low peaks of PA and PF generally appears from southwestern to northeastern Shandong and the PA and PF peaks gradually decrease from southeastern to northwestern Shandong. Moreover, the morning peaks of PA, PI, and PF possibly reflect an effect of the southwest monsoon while their afternoon peaks may indicate an effect of local convection activities triggered by solar radiation heating. However, it is still not clear why the afternoon PI peak has a little influence on PA in the southwestern plain. This should be addressed in the future work.

Acknowledgements

We thank Prof. Lianshou Chen, Drs. Haoming Chen, and Jianzhong Wang for their help. We also thank two anonymous reviewers for their helpful and careful reviews that

greatly improved the manuscript. This work is jointly supported by the National Natural Science foundation of China (41221064) Special project of National International Science and Technology Cooperation of China (2011DFG23450), and the National Key Basic Research Project of China (2009CB421404).

References

Betts AK, Jakob C. 2002. Study of diurnal cycle of convective precipitation over Amazonia using a single column model. *Journal of Geophysical Research* **107**: 4732. DOI: 10.1029/2002JD002264

Chang CP, Wang Z, McBride J, Liu CH. 2005. Annual cycle of Southeast Asia–Maritime Continent rainfall and asymmetric monsoon transition. *Journal of Climate* **18**: 287–301.

Chen H, Yu R, Li J, Yuan W, Zhou TJ. 2010. Why nocturnal long-duration rainfall presents an eastward delayed diurnal phase along the Yangtze River. *Journal of Climate* **23**: 905–917.

Dai A. 2001a. Global precipitation and thunderstorm frequencies. Part I: seasonal and interannual variations. *Journal of Climate* **14**(66): 1092–1111.

Dai A. 2001b. Global precipitation and thunderstorm frequencies. Part II: diurnal variations. *Journal of Climate* **14**(66): 1112–1128.

Dai A, Trenberth KE. 2004. The diurnal cycle and its depiction in the community climate system model. *Journal of Climate* **17**: 930–951.

Dai A, Trenberth KE, Karl TR. 1999a. Effects of clouds, soil moisture, precipitation, and water vapor on diurnal temperature range. *Journal of Climate* **12**: 2451–2473.

Dai A, Giorgi F, Trenberth KE. 1999b. Observed and model simulated diurnal cycles of precipitation over the contiguous united states. *Journal of Geophysical Research* **104**: 6377–6402.

Dai A, Lin X, Hsu KL. 2007. The frequency, intensity, and diurnal cycle of precipitation in surface and satellite observations over low- and mid-latitudes. *Climate Dynamics* **29**: 727–744.

DeMott CA, Randall DA, Khairoutdinov M. 2007. Convective precipitation variability as a tool for general circulation model analysis. *Journal of Climate* **20**: 91–112.

He HZ, Zhang FQ. 2010. Diurnal variations of warm-season precipitation over northern China. *Monthly Weather Review* **138**: 1017–1025.

Li J, Yu R, Zhou T. 2008. Seasonal variation of the diurnal cycle of rainfall in the southern contiguous China. *Journal of Climate* **21**: 6036–6043.

Liang XZ, Li L, Dai A, and Kunkel KE. 2004. Regional climate model simulation of summer precipitation diurnal cycle over the United States. *Geophysical Research Letters* **31**: L24208. DOI: 10.1029/2004GL021054.

Lin X, Randall DA, Fowler LD. 2000. Diurnal variability of the hydrologic cycle and radiative fluxes: comparisons between observations and a GCM. *Journal of Climate* **3**(23): 4159–4179.

Qian JH. 2008. Why precipitation is mostly concentrated over islands in the maritime continent. *Journal of Atmospheric Sciences* **65**: 1248–1441.

Qian T, Dai A, Trenberth KE, Oleson KW. 2006. Simulation of global land surface conditions from 1948–2004. Part I: Forcing data and evaluation. *Journal of Hydrometeorology* **7**: 953–975.

Qian JH, Robertson AW, Moron V. 2010. Interactions among ENSO, the monsoon, and diurnal cycle in rainfall variability over Java, Indonesia. *Journal of Atmospheric Sciences* **67**: 3509–3524.

Sun J, Zhang F. 2012. Impacts of mountain–plains solenoid on diurnal variations of rainfalls along the Mei-Yu front over the east China plains. *Monthly Weather Review* **140**: 379–397.

Sun Y, Solomon S, Dai A, Portmann RW. 2006. How often does it rain? *Journal of Climate* **19**: 916–934.

Sun Y, Solomon S, Dai A, Portmann RW. 2007. How often will it rain? *Journal of Climate* **20**: 4801–4818.

Tao S, Chen L. 1987. A review of recent research on the East Asian summer monsoon in China. In *Monsoon Meteorology, Monographs on Geology and Geophysics*, Vol. **7**, Chang CP, Krishnamurti TN (eds). Oxford University Press: Oxford.

Trenberth KE, Dai A, Rasmussen RM. 2003. The changing character of precipitation. *Bulletin of the American Meteorological Society of Japan* **84**: 1205–1217.

Yang GY, Slingo J. 2001. The diurnal cycle in the tropics. *Monthly Weather Review* **129**: 784–801.

Yin S, Li W, Chen D, Jeong J-H, Guo W. 2011. Diurnal variations of summer precipitation in the Beijing area and the possible effect of topography and urbanization. *Advances in Atmospheric Sciences* **28**(4): 7–41.

Yu R, Zhou T Xiong A, Zhu Y, Li J. 2007a. Diurnal variations of summer precipitation over contiguous China. *Geophysical Research Letters* **34**: L01704, DOI: 10.1029/ 2006GL028129.

Yu R, Xu Y, Zhou T, Li J. 2007b. Relation between rainfall duration and diurnal variation in the warm season precipitation over central eastern China. *Geophysical Research Letters* **34**: L13703. DOI: 10.1029/2007GL030315.

Yuan W, Yu R, Chen H, Li J, Zhang M. 2010. Subseasonal characteristics of diurnal variation in summer monsoon rainfall over central eastern China. *Journal of Climate* **23**: 6684–6695.

Zhao P, Zhang RH, Liu JP, Zhou XJ, He JH. 2007. Onset of southwesterly wind over eastern China and associated atmospheric circulation and rainfall. *Climate Dynamics* **28**: 797–811.

Zhou T, Yu R. 2005. Atmospheric water vapor transport associated with typical anomalous summer rainfall patterns in China. *Journal of Geophysical Research* **110**: D08104. DOI: 10.1029/2004JD005413.

Zhou T, Yu R, Chen H, Dai A, Pan Y. 2008. Summer precipitation frequency, intensity, and diurnal cycle over China: A comparison of satellite data with raingauge observations. *Journal of Climate* **21**(16): 3997–4010.

Zhou T, Gong D, Li J, Li B. 2009. Detecting and understanding the multi-decadal variability of the East Asian Summer Monsoon-Recent progress and state of affairs. *Meteorologische Zeitschrift* **18**(4): 455–467.